Nano World Journal

https://doi.org/10.17756/nwj.2023-s2-077

Research Article

Open Access

$Pb_{0.93}Co_{1.86}Cr_{1.14}(PO_4)_3$: A Novel Non-stochiometric Phosphate with α-$CrPO_4$-type Structure

Fouad Alloun*, Siham El Maataoui, Mohammed Hadouchi, Jamal Khmiyas, Abderrazzak Assani, Mohamed Saadi and Lahcen El Ammari

Laboratoire de Chimie Appliquée des Matériaux, Centre des Sciences des Matériaux, Faculty of Science, Mohammed V University in Rabat, Avenue Ibn Battouta, BP 1014, Rabat, Morocco

***Correspondence to:**

Fouad Alloun
Laboratoire de Chimie Appliquée des Matériaux,
Centre des Sciences des Matériaux,
Faculty of Science,
Mohammed V University in Rabat,
Avenue Ibn Battouta, BP 1014,
Rabat, Morocco.
E-mail: fouad.alloun@um5r.ac.ma

Received: July 25, 2023
Accepted: September 27, 2023
Published: September 29, 2023

Citation: Alloun F, El Maataoui S, Hadouchi M, Khmiyas J, Assani A, et al. 2023. $Pb_{0.93}Co_{1.86}Cr_{1.14}(PO_4)_3$: A Novel Non-stochiometric Phosphate with α-$CrPO_4$-type Structure. *NanoWorld J* 9(S2): S455-S459.

Published by United Scientific Group

Abstract

Transition metal-based phosphates have attracted considerable attention since the study of the electrochemical activity of lithium iron phosphate in batteries by Goodenough's group in 1997. The development of new phosphates with novel structures and the study of their structure-property relationship has been the main subject of several research groups. In this spirit, a novel non-stochiometric phosphate $Pb_{0.93}Co_{1.86}Cr_{1.14}(PO_4)_3$ is synthesized as a single crystal from a melted mixture and its structure is determined by X-ray diffraction technique. The structural determination has shown that it crystallizes in the orthorhombic system with the *Imma* (No. 74) space group. The crystal structure of this phosphate belongs to the α-$CrPO_4$ family which consists of $(Co/Cr)O_6$ octahedra and PO_4 tetrahedra sharing edges and/or vertices to build a 3D (Three-dimensional) framework that contains two distinct tunnels parallel to [100] and [010] where the Pb^{2+} cations are located.

Keywords

Phosphate, Single crystal growth, Crystal structure, α-$CrPO_4$-type structure

Introduction

The synthesis and characterization of metal-based phosphates have been the subject of wide research over the past decades. Despite the fact that many studies on phosphates were reported, there is still much to explore in this field, which has recently been the topic of practical and theoretical works. Metal-based phosphates exhibit interesting electrical [1-3] and magnetic properties [4-6]. In addition, they can be used as photoluminescent materials [7] or as cathodes or anodes for rechargeable batteries [8, 9]. In fact, this variety of properties is related to the nature of cations composing the structures as well as the linkage of basic unit PO_4 tetrahedra with $[MO_n]$ (n = 4, 5, 6) polyhedra using various types of connections, which reveal 2D or 3D frameworks able to accommodate a large selection of alkali metals and alkaline earth cations.

The search for structures adopting an open framework has gained particular interest due to their potential applications as catalysts and energy storage materials [10, 11]. For instance, the α-$CrPO_4$ family of structure exhibits a 3D framework, made up of octahedra and tetrahedra that share corners and/or edges producing wide tunnels along two different crystallographic directions, in which alkali and alkaline earth cations can be housed [12-15]. In this context, a variety of phosphates have been studied, among them, $NaV_3(PO_4)_3$ [16] and $Na_2Ni_2Fe(PO_4)_3$ [17] were proposed as electrode materials for sodium-ion batteries (SIBs).

In this work, we report on the synthesis and the crystal structure study of a

novel off-stoichiometry phosphate belonging to the α-$CrPO_4$ family of phosphates.

Materials and Methodes

Single crystals synthesis

The precursors lead nitrate ($Pb(NO_3)_2$), cobalt nitrate ($Co(NO_3)_2.6H_2O$), chromium nitrate ($Cr(NO_3)_3.9H_2O$) and phosphoric acid (H_3PO_4) were taken in stoichiometric proportions of Pb:Co:Cr:P = 1:2:3:3. The reagents, $Pb(NO_3)_2$, $Co(NO_3)_2.6H_2O$, and $Cr(NO_3)_3.9H_2O$ were dissolved in distilled water. The required amount of H_3PO_4 was added to the resulting metal nitrate solution. The mixture is slightly heated to evaporate the water. After evaporation was completed, a dark green solid precipitate is obtained and then heated at 300 °C for 24 h before being melted at 1200 °C and held at this temperature for 15 min. It was then slowly cooled at a rate of 5 °C/h. The product obtained contains parallelepiped crystals of dark green color.

Structure determination

Data collection from the single crystal was performed at room temperature on the Bruker X8 APEX diffractometer with monochromatic MoKα radiation using an incident wavelength λ = 0.71073 (Å). APEX2 [18] software was used for data collection and SADABS [19] was used for absorption correction using a semi-empirical multi-scan method. The structure was solved using the direct method and refined using the SHELXT 2014 [20] and SHELXL 2014 [21] programs incorporated into the WinGX program [22]. DIAMOND software [23] was used for the structure drawing. The structure is determined at nanometric scale.

Results and Discussion

The crystal structure determination of this phosphate reveals that it crystallizes in the orthorhombic system with the *Imma* space group and a = 10.4161 (4) Å, b = 13.1683 (5) Å, and c = 6.5389 (2) Å. The asymmetric unit of $Pb_{0.93}Co_{1.86}Cr_{1.14}(PO_4)_3$ contains seven cationic sites of which two are completely occupied by P(1) at (*8g*) and P(2) at (*4e*). The Co and Cr atoms are statistically distributed at two crystallographic sites (*8g*) and (*4b*) with Co1/Cr1 or Co2/Cr2 ratio of 0.863/0.137. Lead cations partially occupy the special position (*4e*) with an occupancy of 93.2%. Noting that, there is a ratio difference between the initial materials (Pb:Co:Cr:P = 1:2:3:3) and the final product of $Pb_{0.93}Co_{1.86}Cr_{1.14}(PO_4)_3$, which can be explained by the occurring of incongruent melting before the crystal growth. Crystal data, data collection, and structure refinement parameters are listed in table 1. Atomic positions, atomic displacement, and geometric parameters are given in table 2, table 3, and table 4, respectively.

The structure of this novel phosphate can be described as a 3D framework built up from PO_4 tetrahedra, [(Co2/Cr2)O_6] octahedra, and [$(Co1/Cr1)_2O_{10}$] dimers with edge-sharing of [(Co1/Cr1)O_6] octahedra (Figure 1). The framework of this structure consists of the association of sheets and chains. The sheet parallel to the *bc* plane is constructed from linkage between [$(Co1/Cr1)_2O_{10}$] dimers and PO_4 tetrahedra through common corners and edges (Figure 2a). On the other hand, the chain parallel to [001] direction is made up by the linkage of [(Co2/Cr2)O_6] octahedra and PO_4 tetrahedra (Figure 2b). The adjacent sheets are further linked by the chains which build the three-dimensional framework containing two distinct tunnels parallel to the *a* and *b* axis, in which cations Pb^{2+} are accommodated (Figure 3).

Table 1: Crystallographic data and structure refinement parameters of $Pb_{0.93}Co_{1.86}Cr_{1.14}(PO_4)_3$.

Crystal data	
Chemical formula	$Pb_{0.93}Co_{1.86}Cr_{1.14}(PO_4)_3$
M_r	646.92
Crystal system, space group	Orthorhombic, *Imma*
Temperature (K)	296
a, *b*, *c* (Å)	10.4161 (4), 13.1683 (5), 6.5389 (2)
V (Å^3)	896.89 (6)
Z	4
Radiation type	Mo *K*α
μ (mm^{-1})	22.78
Data collection	
Diffractometer	Bruker X8
No. of measured, independent and observed [$I > 2\sigma(I)$] reflections	4760, 1071, 1015
R_{int}	0.028
$(\sin \theta/\lambda)_{max}$ (Å^{-1})	0.807
Refinement	
$R[F^2 > 2s(F^2)]$, $wR(F^2)$, *S*	0.026, 0.061, 1.04
No. of reflections	1071
No. of parameters	56
$\Delta\rho_{max}$, $\Delta\rho_{min}$ (e Å^{-3})	2.66, -1.09

In [(Co1/Cr1)O_6] octahedra, the $d_{Co1/Cr1—O}$ distances varies from 2.068 (2) to 2.093 (2) Å, while in [(Co2/Cr2)O_6] octahedra, the $d_{Co2/Cr2—O}$ distances varies from 1.973 (2) to 2.054 (3) Å. Similar Co/Cr—O distances have also been reported in the phosphate $NaCoCr_2(PO_4)_3$ [24] in which the M2 site is evenly occupied by Co and Cr atoms with an average Co/Cr—O distance of 2.029 (3) Å. The average $d_{P—O}$ distances

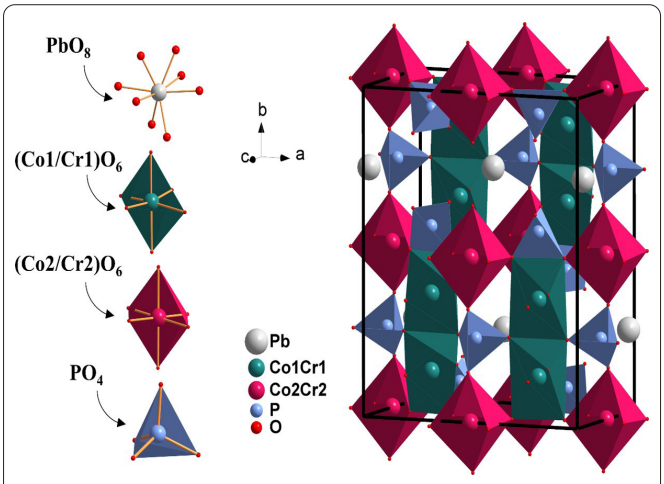

Figure 1: Unit cell representation of $Pb_{0.93}Co_{1.86}Cr_{1.14}(PO_4)_3$ phosphate with polyhedral environments of Pb, Co, Cr, and P atoms.

Table 2: Atomic positions, occupancies, and equivalent displacement parameters.

Atom	*Wyckoff site*	*x*	*y*	*z*	U_{iso}*/U_{eq}	Occ. (<1)
Pb1	*4e*	0.000000	0.250000	0.09998 (4)	0.01974 (10)	0.932
Co1	*8g*	0.250000	0.36737 (4)	0.750000	0.00441 (13)	0.863 (15)
Cr1	*8g*	0.250000	0.36737 (4)	0.750000	0.00441 (13)	0.137 (15)
Cr2	*4b*	0.000000	0.500000	0.500000	0.00194 (16)	0.863 (15)
Co2	*4b*	0.000000	0.500000	0.500000	0.00194 (16)	0.137 (15)
P1	*8g*	0.250000	0.57230 (7)	0.750000	0.00312 (16)	
P2	*4e*	0.000000	0.250000	0.59049 (18)	0.0025 (2)	
O1	*16j*	0.2142 (2)	0.63672 (16)	0.9351 (3)	0.0081 (3)	
O2	*16j*	0.13825 (17)	0.49535 (15)	0.7060 (3)	0.0047 (3)	
O3	*8i*	0.1184 (3)	0.250000	0.7341 (4)	0.0065 (4)	
O4	*8h*	0.000000	0.3455 (2)	0.4577 (4)	0.0071 (5)	

Table 3: Anisotropic displacement parameters.

	U^{11}	U^{22}	U^{33}	U^{12}	U^{13}	U^{23}
Pb1	0.03485 (18)	0.01628 (14)	0.00810 (11)	0.000	0.000	0.000
Co1	0.0040 (2)	0.0027 (2)	0.0065 (2)	0.000	-0.00134 (14)	0.000
Cr1	0.0040 (2)	0.0027 (2)	0.0065 (2)	0.000	-0.00134 (14)	0.000
Cr2	0.0003 (3)	0.0025 (3)	0.0030 (3)	0.000	0.000	0.0006 (2)
Co2	0.0003 (3)	0.0025 (3)	0.0030 (3)	0.000	0.000	0.0006 (2)
P1	0.0032 (4)	0.0025 (4)	0.0036 (3)	0.000	-0.0002 (2)	0.000
P2	0.0015 (5)	0.0026 (5)	0.0033 (5)	0.000	0.000	0.000
O1	0.0082 (8)	0.0077 (8)	0.0083 (7)	0.0019 (7)	0.0014 (6)	-0.0027 (6)
O2	0.0029 (7)	0.0050 (7)	0.0061 (7)	-0.0011 (6)	-0.0016 (6)	0.0006 (5)
O3	0.0031 (11)	0.0098 (11)	0.0065 (10)	0.000	-0.0019 (8)	0.000
O4	0.0070 (11)	0.0060 (12)	0.0083 (11)	0.000	0.000	0.0033 (9)

are 1.547 (3) and 1.539 (2) Å for P1 and P2, respectively. This structure is marked by a partial occupancy of Pb^{2+} which is coordinated by eight neighboring O atoms with a $d_{Pb—O}$ bonds varying from 2.655 (3) to 2.694 (2) Å. Similar coordination for Pb cations was also observed in $PbNi_3(PO_4)_3$ [25] with the α-$CrPO_4$ structure.

Non-stoichiometric compounds, characterized by defects in their crystal structure, such as vacancies or extra atoms, possess unique properties. These defects have a significant influence on various material characteristics, including electrical conductivity, catalytic activity, and optical properties. In addition, non-stoichiometric materials exhibit redox behavior, involving electron transfer between elements. The presence of variable oxidation states facilitates redox reactions, making them valuable as electrode materials in batteries, fuel cells and energy storage devices. Their ability to store and release electrons enables efficient energy conversion and storage [26-28].

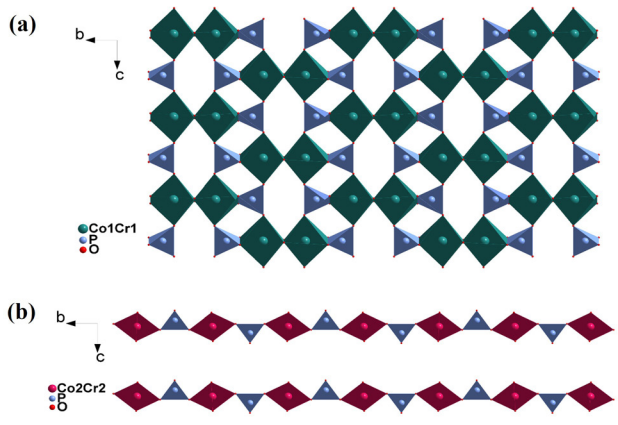

Figure 2: (**a**) $(Co1/Cr1)_2O_{10}$ bioctahedral and PO_4 tetrahedra sharing corners and edges forming sheets. (**b**) Chains of PO_4 tetrahedra and $(Co2/Cr2)O_6$ octahedra with shared corners.

Conclusion

$Pb_{0.93}Co_{1.86}Cr_{1.14}(PO_4)_3$ with α-$CrPO_4$ type structure is elaborated as a single crystal from a melted mixture. It crystallizes in orthorhombic system with the *Imma* space

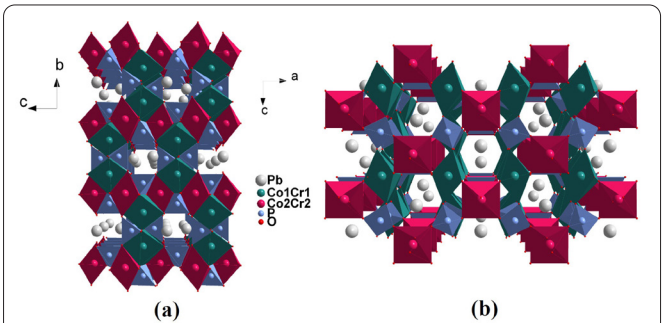

Figure 3: View of the structure along [100] **(a)** and [010] **(b)** with cavities housing Pb cations.

Table 4: Selected interatomic distances (Å) and angels (°).

Distance (Å)			
Pb1—O4^{i}	2.655 (3) × 2	Co1/Cr1—O1$^{x, xi}$	2.093 (2) × 2
Pb1—O3$^{ii, iii}$	2.691 (3) × 2	Co2/Cr2—O2$^{vi, xii, v}$	1.9726 (18) × 4
Pb1—O1$^{iv, v, vi, vii}$	2.694 (2) × 4	Co2/Cr2—O4^{vi}	2.054 (3) × 2
Co1/Cr1—O3^{viii}	2.0683 (18)	P1—O1^{ix}	1.524 (2) × 2
Co1/Cr1—O2	2.0683 (19)	P1—O2^{ix}	1.5700 (19) × 2
Co1/Cr1—O3	2.0683 (18)	P2—O4^{i}	1.528 (3) × 2
Co1/Cr1—O2^{ix}	2.068 (2)	P2—O3^{i}	1.550 (3) × 2
Angle (°)			
O4—Pb1—O4^{i}	56.51 (12)	O2—Co1—O1^{x}	93.31 (8)
O4—Pb1—O3^{ii,}	141.53 (5)	O3—Co1—O1^{x}	84.96 (9)
O4^{i}—Pb1—O3^{ii}	141.53 (5)	O2^{ix}—Co1—O1^{x}	89.10 (8)
O4—Pb1—O3^{iii}	141.53 (6)	O3^{viii}—Co1—O1^{xi}	84.96 (9)
O4^{i}—Pb1—O3^{iii}	141.53 (5)	O2—Co1—O1^{xi}	89.10 (8)
O3^{ii}—Pb1—O3^{iii}	54.56 (11)	O3—Co1—O1^{xi}	92.83 (10)
O4—Pb1—O1^{iv}	109.71 (5)	O2^{ix}—Co1—O1^{xi}	93.31 (8)
O4^{i}—Pb1—O1^{iv}	79.22 (5)	O1^{x}—Co1—O1^{xi}	177.05 (12)
O3^{ii}—Pb1—O1^{iv}	62.91 (6)	O2^{vi}—Co2—O2^{xii}	86.23 (11)
O3^{iii}—Pb1—O1^{iv}	107.69 (6)	O2^{vi}—Co2—O2^{v}	93.77 (11)
O4—Pb1—O1^{v}	79.22 (5)	O2^{xii}—Co2—O2^{v}	180.0
O4^{i}—Pb1—O1^{v}	109.71 (5)	O2^{vi}—Co2—O2	180.0
O3^{ii}—Pb1—O1^{v}	107.69 (6)	O2^{xii}—Co2—O2	93.77 (11)
O3^{iii}—Pb1—O1^{v}	62.91 (6)	O2^{v}—Co2—O2	86.23 (11)
O1^{iv}—Pb1—O1^{v}	170.22 (9)	O2^{vi}—Co2—O4	86.49 (8)
O4—Pb1—O1^{vi}	79.22 (5)	O2^{xii}—Co2—O4	93.51 (8)
O4^{i}—Pb1—O1^{vi}	109.71 (5)	O2^{v}—Co2—O4	86.49 (8)
O3^{ii}—Pb1—O1^{vi}	62.91 (6)	O2—Co2—O4	93.51 (8)
O3^{iii}—Pb1—O1^{vi}	107.69 (6)	O2^{vi}—Co2—O4^{vi}	93.51 (8)
O1^{iv}—Pb1—O1^{vi}	67.25 (9)	O2^{xii}—Co2—O4^{vi}	86.49 (8)
O1^{v}—Pb1—O1^{vi}	111.85 (9)	O2^{v}—Co2—O4^{vi}	93.51 (8)
O4—Pb1—O1^{vii}	109.71 (5)	O2—Co2—O4^{vi}	86.49 (8)
O4^{i}—Pb1—O1^{vii}	79.22 (5)	O4—Co2—O4^{vi}	180.0
O3^{ii}—Pb1—O1^{vii}	107.69 (6)	O1—P1—O1^{ix}	112.38 (17)
O3^{iii}—Pb1—O1^{vii}	62.91 (6)	O1—P1—O2	108.88 (11)
O1^{iv}—Pb1—O1^{vii}	111.85 (9)	O1^{ix}—P1—O2	113.25 (11)
O1^{v}—Pb1—O1^{vii}	67.25 (9)	O1—P1—O2^{ix}	113.25 (11)
O1^{vi}—Pb1—O1^{vii}	170.22 (9)	O1^{ix}—P1—O2^{ix}	108.88 (11)
O3^{viii}—Co1—O2	171.40 (8)	O2—P1—O2^{ix}	99.60 (15)
O3^{viii}—Co1—O3	83.29 (11)	O4^{i}—P2—O4	110.7 (2)
O2—Co1—O3	103.24 (8)	O4^{i}—P2—O3	110.14 (8)
O3^{viii}—Co1—O2^{ix}	103.24 (8)	O4—P2—O3	110.14 (8)
O2—Co1—O2^{ix}	70.87 (10)	O4^{i}—P2—O3^{i}	110.14 (8)
O3—Co1—O2^{ix}	171.40 (8)	O4—P2—O3^{i}	110.14 (8)
O3^{viii}—Co1—O1^{x}	92.83 (10)	O3—P2—O3^{i}	105.4 (2)

Note: Symmetry codes: (i) -x, -y+1/2, z; (ii) -x, -y+1/2, z-1; (iii) x, y, z-1; (iv) -x, y-1/2, -z+1; (v) x, -y+1, -z+1; (vi) -x, -y+1, -z+1; (vii) x, y-1/2, -z+1; (viii) -x+1/2, -y+1/2, -z+3/2; (ix) -x+1/2, y, -z+3/2; (x) x, -y+1, -z+2; (xi) -x+1/2, -y+1, z-1/2; (xii) -x, y, z.

group. The structure is built up via [PO_4] tetrahedra, [(Co2/Cr2)O_6] octahedra and [(Co1/Cr1)$_2O_{10}$] dimers of edge-sharing octahedra, connected through common vertices and/or edges, generating two types of wide channels along the [010] and [100] directions where Pb_{2+} cations are located. The structure of this phosphate is characterized by a partial distribution in the cationic sites.

Acknowledgements

None.

Conflict of Interest

None.

References

1. Rossbach A, Neitzel-Grieshammer S. 2022. Preparation, characterization and conductivity of NASICON-type $Li_{1+x}M^{(III)}_xTi_{2-x}(PO_4)_3$ ($M^{(III)}$ = Al, Cr, Fe; 0.5≤ x≤ 2.0) materials via modern, scalable synthesis routes. *Open Ceram* 9: 100231. https://doi.org/10.1016/j.oceram.2022.100231
2. Saleck AO, Mercier C, Follet-Houttemane C, Assani A, Saadi M, et al. 2022. Two novel phosphates $Na_2Mg_2Fe(PO_4)_3$ and $Ag_2Mg_2Fe(PO_4)_3$ with alluaudite structure: synthesis, crystal structure and electrical properties. *J Solid State Chem* 312: 123139. https://doi.org/10.1016/j.jssc.2022.123139
3. Alloun F, Hadouchi M, Assani A, Saadi M, Lahmar A, et al. 2023. Synthesis, crystal structure, electrical and magnetic properties of a novel phosphate: $Ag_4CoFe_2(PO_4)_4$. *J Solid State Chem* 322: 124006. https://doi.org/10.1016/j.jssc.2023.124006
4. Hadouchi M, Assani A, Saadi M, Saadoune I, Lahmar A, et al. 2018. Synthesis, crystal structure and properties of a new phosphate, $Na_2Co_2Cr(PO_4)_3$. *J Inorg Organomet Polym Mater* 28: 2854-2864. https://doi.org/10.1007/s10904-018-0956-y
5. Saleck AO, Mercier C, Follet C, Mentré O, Assani A, et al. 2020. Synthesis, crystal structure and magnetic behavior of a new calcium magnesium and iron orthophosphate $Ca_2MgFe_2(PO_4)_4$. *J Solid State Chem* 292: 121715. https://doi.org/10.1016/j.jssc.2020.121715
6. Alloun F, Hadouchi M, Assani A, Saadi M, Lahmar A, et al. 2023. Synthesis, structural characterization and magnetic behavior of a novel phosphate: $K_4(Co_{0.25}Fe_{0.75})_4(PO_4)_5$. *Solid State Sci* 139: 107170. https://doi.org/10.1016/j.solidstatesciences.2023.107170
7. Li Z, Lyu Z, Sun D, Shen S, You H. 2022. The downshifting and upconversion photoluminescence from $NaBaSc_2(PO_4)_3$ for multicolor anti-counterfeiting. *Mater Today Chem* 26: 101116. https://doi.org/10.1016/j.mtchem.2022.101116
8. Jenkins T, Alarco JA, Mackinnon ID. 2021. Synthesis and characterization of a novel hydrated layered vanadium(III) phosphate phase $K_3V_3(PO_4)_4.H_2O$: a functional cathode material for potassium-ion batteries. *ACS Omega* 6(3): 1917-1929. https://doi.org/10.1021/acsomega.0c04675
9. Wang X, Hu P, Chen L, Yao Y, Kong Q, et al. 2017. An α-$CrPO_4$-type $NaV_3(PO_4)_3$ anode for sodium-ion batteries with excellent cycling stability and the exploration of sodium storage behavior. *J Mater Chem A* 5(8): 3839-3847. https://doi.org/10.1039/c6ta10862h
10. Natarajan S, Mandal S. 2008. Open-framework structures of transition-metal compounds. *Angew Chem Int Ed* 47(26): 4798-4828. https://doi.org/10.1002/anie.200701404
11. Hadouchi M, Koketsu T, Hu Z, Ma J. 2022. The origin of fast-charging lithium iron phosphate for batteries. *Battery Energy* 1(1): 20210010. https://doi.org/10.1002/bte2.20210010
12. Alhakmi G, Assani A, Saadi M, Follet C, El Ammari L. 2013. $SrMn^{II}_2Mn^{III}(PO_4)_3$. *Acta Cryst Sec E Cryst Commun* 69: i56. https://doi.org/10.1107/S1600536813020977
13. Alhakmi G, Assani A, Saadi M, El Ammari L. 2017. Crystal structures of two alkaline earth (M = Ba and Sr) dimanganese(II) iron(III) tris(orthophosphates). *Acta Cryst Sec E Cryst Commun* 73(5): 767-770. https://doi.org/10.1107/S2056989017006120
14. Assani A, Saadi M, Alhakmi G, Houmadi E, El Ammari L. 2013. $BaMn^{II}_2Mn^{III}(PO_4)_3$. *Acta Cryst Sec E Cryst Commun* 69: i60. https://doi.org/10.1107/S1600536813023106
15. Ouaatta S, Assani A, Saadi M, El Ammari L. 2015. Crystal structure of strontium dinickel iron orthophosphate. *Acta Cryst Sec E Cryst Commun* 71(10): 1255-1258. https://doi.org/10.1107/S205698901501779X
16. Feng P, Wang W, Hou J, Jin Q, Wang K, et al. 2020. The insight into promoting sodium storage mechanism of α-$CrPO_4$-type $NaV_3(PO_4)_3$ anode material for sodium-ion batteries. *J Power Sources* 463: 228194. https://doi.org/10.1016/j.jpowsour.2020.228194
17. Essehli R, Belharouak I, Yahia HB, Chamoun R, Orayech B, et al. 2015. α-$Na_2Ni_2Fe(PO_4)_3$: a dual positive/negative electrode material for sodium ion batteries. *Dalt Trans* 44(10): 4526-4532. https://doi.org/10.1039/c5dt00021a
18. Bruker SAINT-Plus. 2012. Bruker AXS Inc., Madison, Wisconsin, USA.
19. Krause L, Herbst-Irmer R, Sheldrick GM, Stalke D. 2015. Comparison of silver and molybdenum microfocus X-ray sources for single-crystal structure determination. *J Appl Cryst* 48(1): 3-10. https://doi.org/10.1107/S1600576714022985
20. Sheldrick GM. 2015. SHELXT-Integrated space-group and crystal-structure determination. *Acta Cryst Sec A Found Adv* 71(1): 3-8. https://doi.org/10.1107/S2053273314026370
21. Sheldrick GM. 2015. Crystal structure refinement with SHELXL. *Acta Cryst Sec C Struct Chem* 71(1): 3-8. https://doi.org/10.1107/S2053229614024218
22. Farrugia LJ. 2012. WinGX and ORTEP for Windows: an update. *J Appl Cryst* 45(4): 849-854. https://doi.org/10.1107/S0021889812029111
23. Putz H, Brandenburg K. 2018. Diamond-Crystal and Molecular Structure Visualization. Crystal Impact-GbR, Kreuzherrenstr. 102, 53227 Bonn, Germany.
24. Souiwa K, Chennabasappa M, Decourt R, Ben Amara M, Hidouri M, et al. 2015. Novel mixed cobalt/chromium phosphate $NaCoCr_2(PO_4)_3$ showing spin-flop transition. *Inorg Chem* 54(15): 7345-7352. https://doi.org/10.1021/acs.inorgchem.5b00776
25. He Z, Zhang W. 2018. Two successive magnetic transitions observed in a new mixed valence compound $PbNi_3(PO_4)_3$ with channels structure. *J Alloys Compd* 765: 58-62. https://doi.org/10.1016/j.jallcom.2018.06.209
26. Ivanenko AP, Kompanichenko NM, Omelchuk AA, Zinchenko VF, Timukhina EV. 2010. Synthesis and optical properties of non-stoichiometric lanthanide (Sm, Eu, Tm, Yb) fluorides. *Russian J Inorg Chem* 55: 841-847. https://doi.org/10.1134/S0036023610060045
27. Chen P, Zhang L, Wang Z, Wang Y, Song C, et al. 2018. Improved dielectric energy storage performance of Pb-free $0.5Na_{0.5}Bi_{0.5}TiO_3$-$0.5SrTiO_3$ ceramics modified with CaO. *J Adv Dielectr* 8(06): 1850042. https://doi.org/10.1142/S2010135X1850042X
28. Qiao X, Zhang X, Wu D, Chao X, Yang Z. 2018. Influence of Bi nonstoichiometry on the energy storage properties of 0.93KNN-$0.07Bi_xMN$ relaxor ferroelectrics. *J Adv Dielectr* 8(06): 1830006. https://doi.org/10.1142/S2010135X18300062